



**HAL**  
open science

## Developments of methods for improving metal forming operations simulations: Material hardening and friction characterization under process conditions

N. Boudeau, L. Vitu, A. Abdelkefi, P. Malécot, N. Guermazi

### ► To cite this version:

N. Boudeau, L. Vitu, A. Abdelkefi, P. Malécot, N. Guermazi. Developments of methods for improving metal forming operations simulations: Material hardening and friction characterization under process conditions. 30th International Conference on Flexible Automation and Intelligent Manufacturing, FAIM 2021, Jun 2021, Athens, Greece. pp.826-833, 10.1016/j.promfg.2020.10.116 . hal-03159321

**HAL Id: hal-03159321**

**<https://hal.science/hal-03159321>**

Submitted on 25 May 2021

**HAL** is a multi-disciplinary open access archive for the deposit and dissemination of scientific research documents, whether they are published or not. The documents may come from teaching and research institutions in France or abroad, or from public or private research centers.

L'archive ouverte pluridisciplinaire **HAL**, est destinée au dépôt et à la diffusion de documents scientifiques de niveau recherche, publiés ou non, émanant des établissements d'enseignement et de recherche français ou étrangers, des laboratoires publics ou privés.



30th International Conference on Flexible Automation and Intelligent Manufacturing (FAIM2020)  
15-18 June 2020, Athens, Greece.

## Developments of methods for improving metal forming operations simulations: material hardening and friction characterization under process conditions

N. Boudeau<sup>1\*</sup>, L. Vitu<sup>2</sup>, A. Abdelkefi<sup>3</sup>, P. Malécot<sup>1</sup>, N. Guermazi<sup>4</sup>

<sup>1</sup> UBFC/ENSMM, FEMTO-ST UMR CNRS 6174, Besançon, France

<sup>2</sup> UBFC/UTBM, ICB UMR CNRS 6303, Belfort, France

<sup>3</sup> INSA, LGCGM EA 3913, Rennes, France

<sup>4</sup> ENIS, LGME, Sfax, Tunisia

\* Corresponding author. Tel.: +33-381-666-034; fax: +33-381-666-700. E-mail address: [nathalie.boudeau@univ-fcomte.fr](mailto:nathalie.boudeau@univ-fcomte.fr)

### Abstract

Metal forming operations are optimized by using finite element simulations. The numerical results are strongly dependent on the material data and the friction conditions. The present paper focuses on the tube hydroforming process and methods, developed by the authors, for the evaluation, the closest to the process conditions, of the hardening curve and the friction coefficient. For the hardening curve, an experimental set-up has been developed and instrumented, and an analytical model permits to translate the measures into stress-strain curve. Its capability to evaluate the best plastic criterion and its importance for a good prediction of forces during the tube hydroforming are illustrated. For the friction evaluation, the study of tube expansion in a square section die is proposed. By analyzing the thickness along the perimeter of the shaped tube, it is possible to evaluate the Coulomb's friction coefficient, which can be different from the evaluation done with the classical pin-on-disk test.

© 2020 The Authors. Published by Elsevier Ltd.

This is an open access article under the CC BY-NC-ND license (<https://creativecommons.org/licenses/by-nc-nd/4.0/>)

Peer-review under responsibility of the scientific committee of the FAIM 2021.

**Keywords:** Metal forming ; tube hydroforming ; hardening curve ; friction ; experiments ; simulation

### 1. Introduction

Nowadays, all metal forming operations are developed with the use of finite element simulations for reducing the adjustment on press and the time-to-market [1].

Numerous commercial code propose material database for the classical metals worked with forming processes and even, authorize the users to integrate their own material data for the plastic behavior. For the friction conditions, it is often recommended to impose a value in the range of 0.1 – 0.18 for the Coulomb's coefficient with no real physical basis [2].

These data give quite good predictions for simple forming operations and well-known metals, and seem quite well adapted for classical metal forming operations like stamping and deep drawing, certainly due to a large research activity in

this field during the 1980-2000 period. But there is no assurance it is convenient for the new metals [3] and for other metal forming processes like spin forming or tube hydroforming for example [4].

Generally, these material hardening curves and the recommended values for the friction coefficient are obtained with the classical tensile test and the pin-on-disk test respectively, which are not representative of the real loading conditions met by the metal during forming operations [5,6].

The authors propose simple experimental procedures to get the hardening curve and the friction coefficient under experimental conditions very close to the ones met during tube hydroforming. Section 2 presents the tube bulging test and an analytical model to post-process the experimental results to get the hardening curve. Section 3 is devoted to the

2351-9789 © 2020 The Authors. Published by Elsevier Ltd.

This is an open access article under the CC BY-NC-ND license (<https://creativecommons.org/licenses/by-nc-nd/4.0/>)

Peer-review under responsibility of the scientific committee of the FAIM 2021.

10.1016/j.promfg.2020.10.116

characterization of the friction coefficient with the tube expansion test and the Orban-Hu model [7].

**Nomenclature**

$\underline{\varepsilon}$	strain tensor
$\underline{\sigma}$	stress tensor
$\varepsilon_\theta$	circumferential strain
$\varepsilon_\varphi$	longitudinal strain
$\varepsilon_r$	radial strain
$\sigma_\theta$	circumferential stress
$\sigma_\varphi$	longitudinal stress
$\bar{\varepsilon}$	equivalent strain
$\bar{\sigma}$	equivalent stress
$r$	the die radius
$d$	the tube diameter
$t_0$	the initial thickness of the tube
$p$	the internal pressure in the tube
$h$	the bulge height
$t$	the current thickness of the bulged tube
$R$	the curvature of the bulged tube
$y$	the position of the centre of the arc of circumference
$Y$	the Y-coordinate of the points on the arc of circumference representing the bulged tube
$r_c$	the current corner radius
$l_w$	the contact length in the wall
$\varepsilon_c$	the strain in the corner
$F_c$	the friction force
$\mu$	the Coulomb's friction coefficient
TBT	Tube Bulging Test
BM2012	Boudeau-Malécot 2012 model
FE	Finite Element

**2. Material characterization**

In metal forming, the material is subject to biaxial efforts and so, the material behavior cannot be well represented with the standard tensile test. For that, the flange bulging test has been developed and, in parallel, several analytical models have been developed [8]. An extension of this biaxial test has been proposed for tube: the Tube Bulging Test (TBT). In the literature, two main versions exist: ones load the material in expansion with an internal pressure; others combine an internal pressure and axial compressive forces. The seconds are particularly interesting for building Forming Limit Diagrams because it permits to explore different strain paths in the expansion domain. The TBT developed in the following belongs to the first category.

*2.1. The Tube Bulging Test (TBT)*

The Tube Bulging Test (TBT) developed in our lab is represented in Fig. 1. The tube is clamped at its two extremities with a cone-on-cone contact. The conical punch is grooved in order to realize the sealing. One of the punch is drilled to feed the interior of the tube with a fluid under pressure. The tube is guided along its length in a die

presenting a window where the tube can bulge freely. The pressure is measured with the help of a pressure sensor and the bulging of the tube at its central part is measured with a displacement sensor. The resulting experimental curve is a (p,h) curve illustrated in Fig. 2. In our lab, the important dimensions are listed in Table 1.

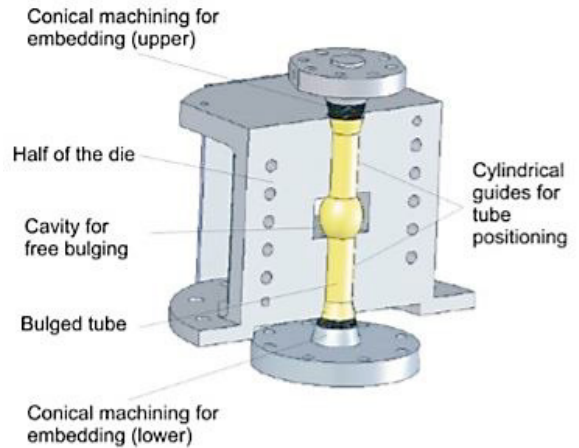


Fig. 1. CAD model of the Tube Bulging Test in the lab.

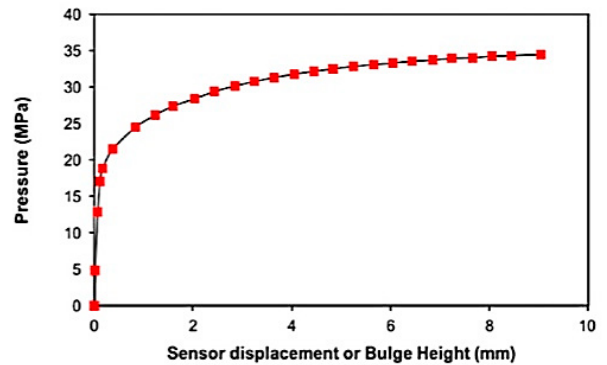


Fig. 2. An example of the resulting (P,h) curve from a TBT.

Table 1. The important dimensions for the TBT in the lab.

Tube length	250 mm
Tube outer diameter	35 mm
Tube thickness	0.5 – 2 mm
Tube free length	50 mm

*2.2. A short review*

Different analytical models exist in the literature to get the stress-strain curve from the (p,h) curve. They all present drawbacks and advantages. Some of them are based on a time and material consuming experimental procedure [11, 14-16]. Others need only one tube and are based on on-line

measurement [9,10,12,13]. For post-processing the experimental (p,h) curve, some need FE simulations to run inverse method for identification and so, need a strong assumption on the hardening law, but no assumption on the shape of the bulged tube [11,12,14]. Others are based on the slice method [9,10,13,15] and then need a geometrical representation of the bulged tube. It is an arc of circumference in [9,10], an arc of ellipse in [13] taking into account the die radius; it is measured in [15] leading to a long experimental procedure. The Hwang model [13] needs to do an additional assumption on the thickness distribution. And, only one is capable to post-process the experimental results to get the stress-strain curve with a spreadsheet (Excel-type) application: it is the Boudeau-Malécot 2012 model [10] for which the theory is developed in Section 1.3. Thus, it constitutes a very interesting “tool” for a use in an industrial context.

2.3. The Boudeau-Malécot 2012 model

For developing the analytical Boudeau-Malécot 2012 model (BM2012), a geometrical parametrization of the bulged tube (Fig. 3) permits the calculation of the strains. The stresses can be evaluated with the help of the slice method, by studying the mechanical equilibrium of two elementary volumes (Fig. 4).

As we consider thin tubes, we can do the hypothesis of plane stress. The tube presents a revolution symmetry, which is respected by the pressure loading. So the strain and stress tensors can be considered as following:

$$\underline{\varepsilon} = \begin{bmatrix} \varepsilon_\theta & 0 & 0 \\ 0 & \varepsilon_\varphi & 0 \\ 0 & 0 & \varepsilon_r \end{bmatrix} \quad \underline{\sigma} = \begin{bmatrix} \sigma_\theta & 0 & 0 \\ 0 & \sigma_\varphi & 0 \\ 0 & 0 & 0 \end{bmatrix} \quad (1)$$

In our study, it was found that  $\varepsilon_\varphi$  was quite constant. Therefore, the strain components at the apex are defined by the following equations:

$$\begin{cases} \varepsilon_\varphi(\varphi) \approx \ln\left(\frac{R \cdot \varphi_{max}}{d}\right) \\ \varepsilon_\theta(\varphi) \approx \ln\left(\frac{Y(\varphi)}{r}\right) \\ \varepsilon_r(\varphi) = -\varepsilon_\varphi(\varphi) - \varepsilon_\theta(\varphi) \end{cases} \quad (2)$$

with:

$$\begin{aligned} R &= \frac{h^2 + d^2}{2h} \\ y &= r + h - R \\ Y(\varphi) &= y + \sqrt{R^2 - [Z(\varphi)]^2} \\ Z(\varphi) &= R \cdot \sin\varphi \\ \varphi_{max} &= \text{asin}\left(\frac{d}{R}\right) \end{aligned} \quad (3)$$

The mechanical equilibrium of the elementary volumes of Fig. 5 gives:

$$\begin{cases} t(\varphi) \cdot Y(\varphi) \cdot \cos\varphi \cdot \sigma_\varphi(\varphi) - \frac{1}{2} p \cdot [Y(\varphi)]^2 = C \\ \frac{\sigma_\theta(\varphi)}{Y(\varphi)} + \cos\varphi \cdot \frac{\sigma_\varphi(\varphi)}{R} = \frac{p}{t(\varphi)} \end{cases} \quad (4)$$

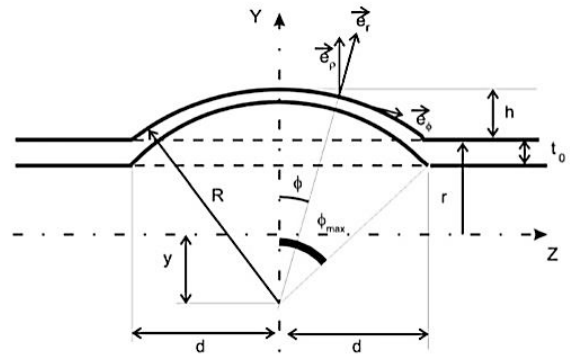


Fig. 3. Parametrization of the Tube Bulging Test

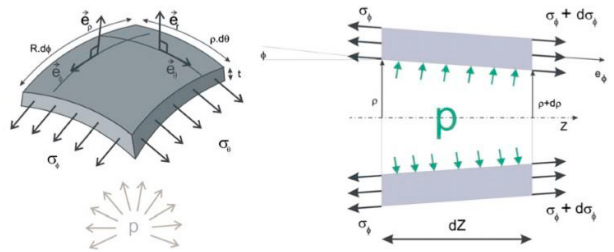


Fig. 4. The mechanical equilibrium of two infinitesimal representative volumes.

To get the constant C, it is necessary to consider the equilibrium of a half longitudinal slice of the bulged tube illustrated in Fig. 5. The longitudinal stress at the pole can be found to be equal to:

$$\sigma_\varphi(\varphi = 0) = \frac{p}{t(0)} \cdot \left( h + \frac{d}{\tan\varphi_{max}} \right) \quad (5)$$

When the curvature is very weak, corresponding to a very small deformation of the tube, Eq. (5) leads to numerical problem and it is necessary to define the  $\varphi$  angle which can do the distinction between enough or not enough curvature:

$$\varphi_{max}^{lim} = \text{atan}\left(\frac{2d}{r-h}\right) \quad (6)$$

Taking into account Eq. (4-6), the C constant is defined by:

$$\begin{aligned} \text{if } \varphi < \varphi_{max}^{lim} \quad C &= 0 \\ \text{else } C &= t(0) \cdot (r + h) \cdot \sigma_\varphi(0) - \frac{1}{2} \cdot p \cdot (r + h)^2 \end{aligned} \quad (7)$$

When  $C = 0$ ,  $\sigma_\varphi(\varphi = 0) = pr/2t$  corresponding to the longitudinal stress of a tube closed at its extremities, under an internal pressure.

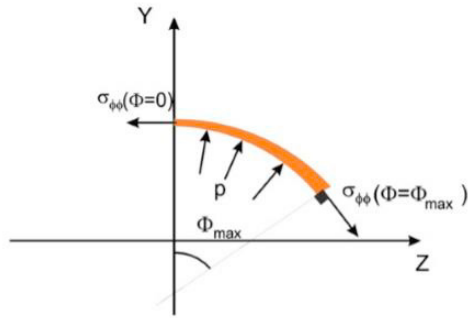


Fig. 5. Model the equilibrium of a half longitudinal slice of the bulged tube for the C constant evaluation.

2.4. Results and discussion

The first step is to validate the model. The experimental procedure proposed in [9] is conducted. FE simulations of the TBT are run with an imposed hardening curve. The global results (p,h) obtained with the simulation are post-processed with the model, in place of the experimental ones. The results corresponding to the reference configuration (Ref. Config. in Fig. 7) show the good capability of the BM2012 to get the stress-strain curve from the TBT.

The full analytical model (BM2012) is compared to the Hwang’s model. The experimental procedure is the same for these two models: 1 tube, 1 test, 1 (p,h) curve without FE simulations. Their sensitivity to the configuration of the TBT is studied. Table 2 gives the different studied configurations, and the resulting flow curves obtained with BM2012 are given in Fig. 6. The Hwang’s model presents less scattering than BM2012, especially for the smaller free bulge length and for the larger die radius. With respect to St Venant’s principle, for a given free length, more the radius is large, more its influence is important; in the same way, for a given die radius, more the free length is short, more the influence of the die radius is important. Because the Hwang’s model takes into account the die radius in its mathematical developments, it is less sensitive to the test configuration. Table 3 permits a comparative analysis of the sensitivity to the TBT configuration for the two models, and it can be observed a very good capability of the full-analytical BM2012 to get the  $(\bar{\sigma}, \bar{\epsilon})$  curve from the (p,h) curve.

The main interest of these models is that no hypothesis is made on the hardening law. Moreover, they permit to evaluate the components of the strain and stress tensors and then, different plastic criteria (see Appendix A) can be studied to define the hardening curve, meaning the  $(\bar{\sigma}, \bar{\epsilon})$  curve, as it is illustrated in Fig. 7. It would permit, by further analyses (inverse method for example), to define the best plastic criterion for representing the plastic behavior of tubular materials.

By the way, the comparison of plastic flow curve for a 304 stainless steel obtained with a tensile test and a TBT shows clearly a very different behavior (Fig. 8). These two hardening curves have been used to simulate a tube hydroforming process (Fig. 9). Fig. 8 shows that the material behavior obtained with the classical tensile test presents a higher

rigidity and a lower ductility than with the TBT. The maximal stress is around 800 MPa for a maximal strain of less than 0.2. With the TBT, the maximal stress is evaluated to 550 MPa and the maximal strain is 0.25. These differences of plastic flow will lead to an overestimation of the needed pressure to obtain the desired shape of the hydroformed part. From the results presented in Fig. 9, if the desired hydroformed part corresponds to the reference displacement of 1 mm, it will give an effort on the tools of 480 kN or 425 kN depending we use the hardening law obtained with the tensile test or the TBT respectively. This loading difference represents an overestimation of around 15% and then, to an overdimensioning of the tools leading to the generation of overcost for the company. The comparison with the experimental measures show clearly than the hardening curve obtained with the TBT gives process efforts closer to the measures.

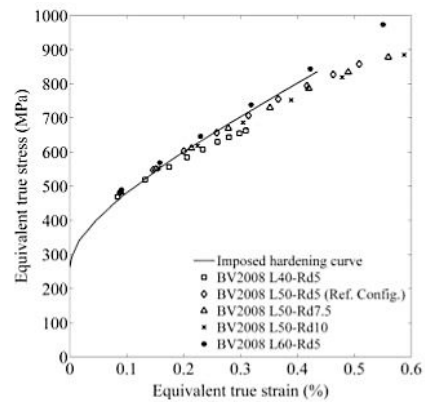


Fig. 6. Hardening curve obtained by post-processing the (p,h) curve with the Boudeau-Malécot 2012 model (from [15]).

Table 2. The different configurations of the TBT.

Configurations	Free bulging length L (mm)	Die radius Rd (mm)
L40-Rd5	40	5
L50-Rd5 (Ref. Config.)	50	5
L50-Rd7.5	50	7.5
L50-Rd10	50	10
L60-Rd5	60	5

Table 3. Deviations between models and reference

Data	Ref	Model	Min %	Max %
$\epsilon_\theta$	FE	Hwang	+1.6	+1.8
		BM 2012	-2.6	-2.4
$\epsilon_\phi$	FE	Hwang	-3100	+2041
		BM 2012	-387	+649
$\epsilon_r$	FE	Hwang	-31.5	-10.6
		BM 2012	+2.5	+4
$\sigma_\theta$	FE	Hwang	-5.2	-1.1
		BM 2012	-0.7	+5.4
$\sigma_\phi$	FE	Hwang	-9.8	+8.4
		BM 2012	+0.6	+19.6

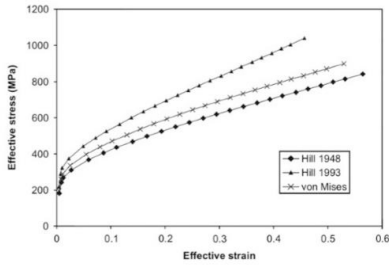


Fig. 7. The resulting  $(\bar{\sigma}, \bar{\epsilon})$  curve for different plastic criteria

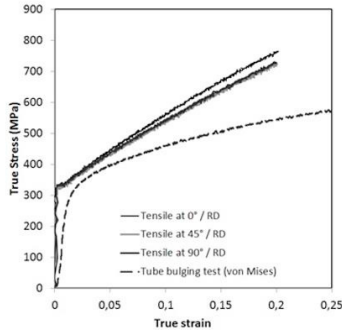


Fig. 8. Comparison of the plastic flow curve obtained with the tensile test and the TBT

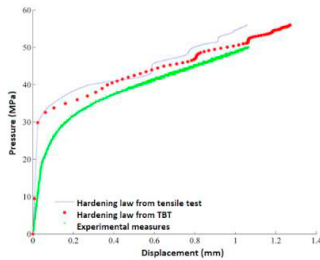


Fig. 9. Estimation of hydroforming forces in tube hydroforming process with the flow curves obtained with the tensile test or the TBT.

### 3. Friction testing for tube hydroforming

Friction is generally evaluated with the pin-on-disk test which is not representative of the friction conditions during the tube hydroforming process. Several tests have been developed for the evaluation of friction in the guiding zone, or in the expansion zone [6]. We concentrate in the present paper on the friction conditions in the expansion zone and we consider the analytical model developed by Orban-Hu [7]. In section 3.1, the theory of the selected model is shortly presented. Its validation is proposed in section 3.2 and results are presented in section 3.3.

#### 3.1. Theory of the Orban-Hu model

“The Orban-Hu model [9] deals with the corner filling in tube hydroforming in a square die. It considers two distinctive parts named the corner and the wall as represented in Figure 10. Mechanical equilibrium of the corner is only related to the internal pressure. For the wall, tangential forces, due to

friction effect, are also taken into account; moreover, stick and slip conditions are considered. With this mathematical model, it is then possible to evaluate the evolution of the corner radius, wall length, corner thickness and thickness along the wall within the internal pressure. Its theoretical development has been possible by considering the material following a Swift hardening law.

The Orban-Hu model can be solved with the following set of equations:

$$\begin{bmatrix} 2 - \frac{\pi}{2} & 2 \frac{\pi r_c}{2} & 0 \\ -p & 0 & 0 & 1 \\ 0 & 0 & 1 & -\beta_c \\ 0 & 1 & 0 & -c_2 \end{bmatrix} \begin{bmatrix} \Delta r_c \\ \Delta l_w \\ \Delta \epsilon_c \\ \Delta F_c \end{bmatrix} = \begin{bmatrix} 0 \\ r_c \cdot \Delta p \\ 0 \\ c_1 \cdot \Delta p \end{bmatrix} \quad (8)$$

where  $\Delta p$  is the incremental in internal pressure,  $r_c$  the current thickness of the tube,  $\beta_c$  a parameter linked to the current corner thickness and the current slope of the hardening curve,  $c_1$  and  $c_2$  two “constants” which depends on the friction coefficient, the current internal pressure, the current slope to the hardening curve and the increase in length of the contact surface in the wall area  $l_w$ .

The Orban-Hu model has been programmed with Matlab© and validated with results presented in their paper [7].” (from [18]). The input data are the square side (target for the final shape of the hydroformed tube), the values of the Swift’s law parameters, the friction coefficient and the final pressure. The resolution of the set of equations Eq. (8) permits to calculate the increase of the corner radius  $\Delta r$ , the contact length in the wall  $\Delta l_w$ , the strain in the corner  $\Delta \epsilon_c$  and the friction force  $\Delta F_c$ . The knowledge of the friction force  $F_c$  gives the Coulomb’s friction coefficient  $\mu$ .

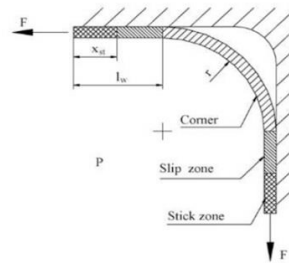


Fig. 10. Model for the development of the Orban-Hu model (from [18])

#### 3.2. Validation of the Orban-Hu model

The Orban-Hu model has been programmed with Matlab© and validated with results presented in their paper [7]. We propose other validations using FE simulations.

The tube expansion in a square section die is modeled with FE simulations using Ls Dyna© software for a referent tube with the following geometry: a 35 mm external diameter and a 1 mm initial thickness, corresponding to a configuration adapted to our experimental device. A referent material, represented by the following Swift law, has been used to run FE simulations and the Orban-Hu model:

$$\sigma_0(\bar{\epsilon}^p) = 263.63 (0.0043 + \bar{\epsilon}^p)^{0.287} \text{ (MPa)} \quad (9)$$

Different FE models are considered; they are listed in Table 4 and illustrated in Fig.11. For the 3D solid model, 3D solid fully integrated quadratic 8-nodes elements are used.

Table 4. Description of the studied FE models (FEM means “finite element model”, EL means “element” and IP means “integration point”)

Models	Type of FEM	Details	Total EL
2D_2E	2D plane strain	2 EL/thickness	108
2D_4E	2D plane strain	4 EL/thickness	432
3D shell	3D shell	5 IP/thickness	53500
3D solid_4E	3D solid	4 EL/thickness	52000

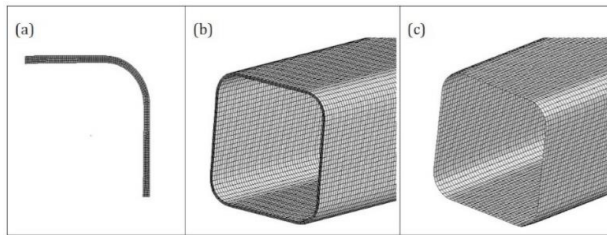


Fig. 11. The final shape of the tube hydroformed in a square section die obtained with different FE models (a) 2D plane strain (b) 3D shell (c) 3D solid

In reference to [7], the following results have been compared:

- The corner thickness  $t_c$  vs. the corner radius
- The wall length vs. the internal pressure
- The corner radius vs the internal pressure

The thickness distribution along the perimeter of the shaped tube is also studied and illustrated in Fig. 12.

The comparison between results obtained with the FE models and with the analytical model are summarized in Table 5 where the adopted rating is from -2, for a very weak correlation, to +2, for a good correlation.

It appears from the decision matrix of Table 5 that the 3D shell and 3D solid FE models are the most appropriate to study the friction behavior. The 3D shell model will be privileged as it needs less computation time to get the results and seems better to get the thickness repartition (Fig. 12).

The Orban-Hu model permits to model the main behavior of the tube expansion in a closed die due to the friction conditions. Next section will study the way we could use it for the evaluation of the friction coefficient in tube hydroforming.

Table 5. Summary of correlation between FE results and the analytical results obtained with the Orban-Hu model.

	2D_2E	2D_4E	3D shell	3D solid_4E
$t_c$ vs. $r_c$	-2	+2	-1	+1
$l_w$ vs. $p$	-2	-2	+1	+2
$r_c$ vs. $p$	-2	-2	+2	+2
Fig. 12	-2	-2	+2	-1
<b>Summary</b>	<b>-8</b>	<b>-4</b>	<b>+4</b>	<b>+4</b>

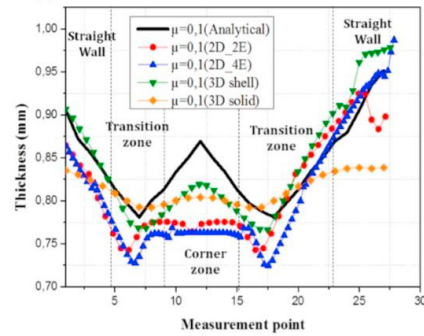


Fig. 12. The thickness repartition along the perimeter of the shaped tube obtained with the Orban-Hu model and with the different FE models

### 3.3. Evaluation of friction coefficient

From section 3.2, the thickness distribution along the perimeter of the shaped tube seems an interesting characteristic for the Coulomb’s friction coefficient. We will focus on such a characteristic for evaluating the friction conditions.

For that, FE simulations and experiments are carried out on Copper tubes with a 250 mm total length, a 35 mm external diameter and a 0.9 mm initial thickness.

The square section die is centered on the tube with a square section of 35 mm side, a 60 mm length and 5 mm fillet radii.

We have characterized the plastic behavior of the Copper tube material with the TBT and its representative Swift’s law is given below:

$$\sigma_o(\bar{\epsilon}^p) = 441.97(0.0075 + \bar{\epsilon}^p)^{0.349} \text{ (MPa)} \quad (10)$$

Experiments are conducted with and without lubricant. The distribution of thickness along the perimeter of the transversal section of the tube is measured and is represented in Fig. 13. It shows the capability of the expansion test in a square die to reveal the effect of the friction conditions. The results are analyzed in Table 6 where it can be affirm that:

- The presence of lubricant leads to a repartition of thickness more uniform along the tube perimeter
- The lack of lubricant leads to a more important thinning in the corner
- The transition zone is the location of an important thinning even the test is run with or without lubricant

Table 6. Analysis of experimental results presented in Fig. 13 (initial thickness is 0.9 mm)

	Without lubricant	With lubricant
Maximal thickness	0.85	0.84
Minimal thickness	0.69	0.72
Delta thickness	0.16	0.12
Thickness in the corner	0.82	0.84
Thickness in the wall	0.815	0.84
Thickness in the transition zone	0.69-0.71	0.72-0.73

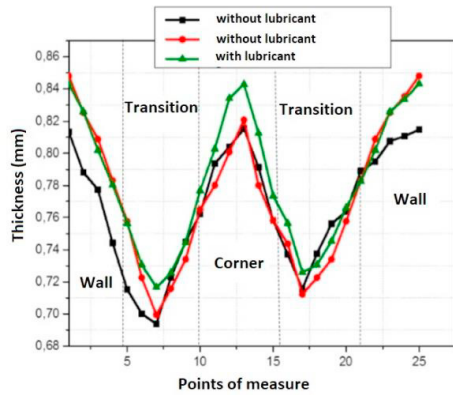


Fig. 13. Thickness distribution measured in tube expansion in a square section die performed with and without lubricant

The experimental results have been compared to results obtained with the Orban-Hu model for different friction coefficients in Fig. 14 and from it, it could be concluded that a friction coefficient of 0.5 is the more representative of the friction conditions. With the pin-on-disk test, it was evaluated to 0.1 in the same lubricant conditions. The values of the friction coefficient are very different for the two testing methods. The differences can be explained by the very different experimental conditions:

- For the pin-on-disk test, a 100Cr6 ball rolls during 1 hour, with a rotation rate of 150 turns per minute and loaded with a normal force of 2 or 5 N, on a Copper disk with back-and-forth trips. So, the movement of the contactor is a rotation. Considering the 100Cr6 steel and the classical theory of contact, we can evaluate the contact pressure of about 1500 and 2000 MPa. This pressure is constant during the whole test.
- For the tube expansion in a square section die, the pressure at the contact is the internal pressure limited to 28 MPa at its maximum. The contact zone is progressive with the deformation of the tube. There is very few relative displacement between the contactor and the tube.

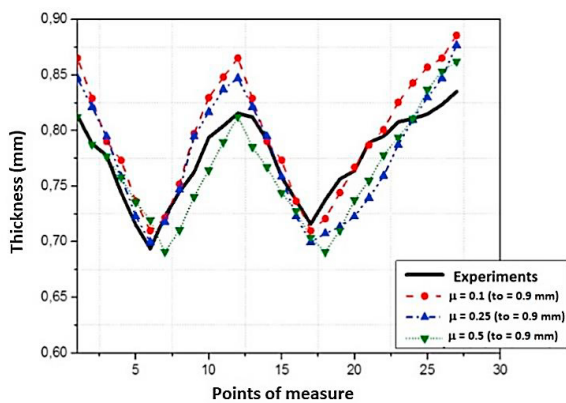


Fig. 14. The thickness repartition along the perimeter of the shaped tube obtained with the Orban-Hu model for different friction coefficients and compared to the experimental measures

The analysis of the thickness distribution along the perimeter of the shaped tube can be relatively complex. Moreover, the analysis of the figures presented in Table 6 and visible in Fig. 13 reveals that the thickness amplitude along the tube perimeter seems more discriminatory than the minimal thickness:

- The study of the evolution of the minimal thickness between the tests run with or without lubricant shows a variation of about 4%
- The same study based on the thickness amplitude gives a variation of about 30%

Thus, we propose the study of these two characteristics, meaning the thickness variation and the minimal thickness.

For that, the Orban-Hu model is run with different friction coefficients for tube with different thicknesses. The thickness variation and the minimal thickness in the perimeter of the deformed tube obtained for the different friction coefficients and a given loading condition are illustrated in Fig. 15 and Fig. 16. Finally, the variation thickness is not a so discriminatory measure as the resulting curves are very close to each other for different thicknesses (Fig. 15). In the contrary, the minimal thickness is more selective (Fig. 16) and could be used to estimate the friction coefficient. For a tube of 0.9 mm and a given pressure, the minimum thickness is searched in the specimen. It is marked in the graphic as it is shown in Fig. 17 permitting to evaluate the friction coefficient to be equal to about 0.4, closer to the quick evaluation done from Fig. 14 than the one given by the pin-on-disk test.

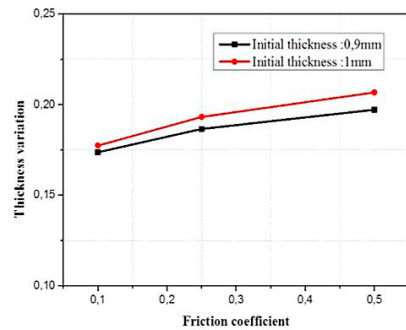


Fig. 15. The resulting thickness variation along the tube perimeter for different friction coefficients and different initial tube thickness. The results are obtained with the Orban-Hu model.

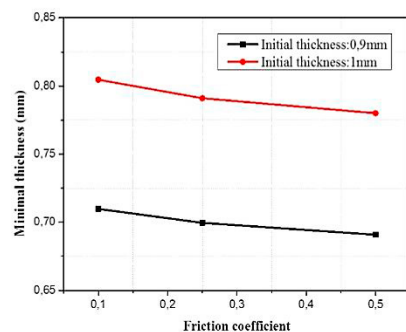


Fig. 16. The resulting minimal thickness along the tube perimeter for different friction coefficients and different initial tube thickness. The results are obtained with the Orban-Hu model

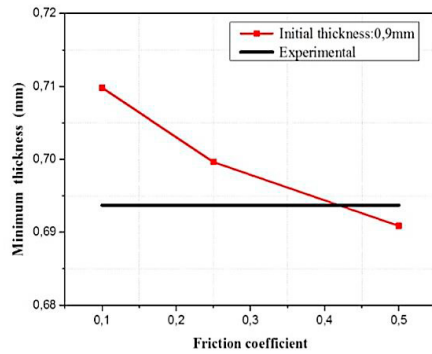


Fig. 17. Graphic evaluation of the friction coefficient value with the minimal thickness curve

#### 4. Conclusion

The present paper focuses on the characterization of two important data for the simulation of the tube hydroforming process: the plastic flow curve and the friction coefficient. The main and common goal is to propose experimental procedure and analytical models, which can be easily implement in an industrial context.

For the hardening curve, the TBT is proposed and a simple experimental procedure is defined where experimental measures are obtained on-line with a very simple instrumentation based on a pressure and a displacement sensors. In parallel, a full-analytical model permits to treat the experimental measures to get the stress-strain curve with a spreadsheet application generally available in the devoted industrial services. The results are very satisfying: no assumption on the material model for the hardening and the plastic criteria. Simulations done with this characterization lead to better evaluation of the process parameters (ie. the maximal internal pressure to get the good shape).

For friction evaluation, the tube expansion in a square section die is proposed associated with the Orban-Hu analytical model. The procedure can be easily carried out in a measurement industrial service. The results show that the tube expansion in a square section die is an interesting test: the friction conditions lead to different final part in terms of thickness repartition. And, for high friction conditions, the final part presents a large variation in thickness. A procedure, based on the analysis of the minimum thickness, is proposed. It permits to evaluate the friction coefficient, which is very different from the one given by the classical pin-on-disk test.

#### Appendix A. Plastic criteria

The plasticity criteria used in section 2.4 and Fig. 7 are:

- The von Mises criterion:

$$\bar{\sigma}^2 = \sigma_\theta^2 + \sigma_\phi^2 - \sigma_\theta \sigma_\phi$$

- The Hill 1948 criterion:

$$\bar{\sigma}^2 = \sigma_\phi^2 - c \cdot \sigma_\theta \sigma_\phi + a \cdot \sigma_\theta^2$$

- The Hill 1993 criterion:

$$\bar{\sigma}^2 = \sigma_\theta^2 - c \cdot A \cdot \sigma_\theta \sigma_\phi + [(p + q) - B \cdot \sigma_\theta - C \cdot \sigma_\phi] \cdot \sigma_\theta \sigma_\phi$$

where  $a, c, p, q, A, B, C$  are plastic characteristics.

The equivalent plastic strain is evaluated with the following relation:

$$\bar{\epsilon} \cdot \bar{\sigma} = \epsilon_\theta \sigma_\theta + \epsilon_\phi \sigma_\phi$$

#### References

- [1] Hattalli VL., Srivatsa SR, Sheet Metal Forming Processes – Recent Technological Advances, Materials Today: Proceedings 5 (2018) 2564–2574
- [2] LS Dyna Examples manual June 2001 ([http://ftp.lstc.com/anonymous/outgoing/jday/manuals/ls-dyna\\_examples\\_manual.pdf](http://ftp.lstc.com/anonymous/outgoing/jday/manuals/ls-dyna_examples_manual.pdf)) visited on the 03/02/2020
- [3] Nasser A, Yadav A, Pathak P, Altan T, Determination of the flow stress of five AHSS sheet materials (DP 600, DP 780, DP 780-CR, DP 780-HY and TRIP 780) using the uniaxial tensile and the biaxial Viscous Pressure Bulge (VPB) tests, Journal of Materials Processing Technology 210 (2010) 429-436
- [4] Lang LH et al., Hydroforming highlights: sheet hydroforming and tube hydroforming, Journal of Materials Processing Technology 151 (2004) 165-177
- [5] Jansson M, Nilsson L, Simonsson K, The use of biaxial test data in the validation of constitutive descriptions for tube hydroforming applications, Journal of Materials Processing Technology 184 (2007) 69-76
- [6] Vollersten F, Plancak M, On possibilities for the determination of the coefficient of friction in hydroforming of tubes, Journal of Materials Processing Technology 125–126 (2002) 412-420
- [7] Orban H, Hu SJ, Analytical modeling of wall thinning during corner filling in structural tube hydroforming, Journal of Materials Processing Technology, 194 (2007) 7-14
- [8] Koç M, Billur E, Necati Cora O, An experimental study on the comparative assessment of hydraulic bulge test analysis methods, Materials and Design 32 (2011) 272-281
- [9] Velasco R, Boudeau N, Tube bulging test: theoretical analysis and numerical validation, Journal of Materials Processing Technology 205 (2008) 81-59
- [10] Boudeau N, Malécot P, A simplified analytical model for post-processing experimental results from tube bulging test: theory, experimentations, simulations, International Journal of Mechanical Sciences 65 (2012) 1-11
- [11] Sokolowski T et al., Evaluation of tube formability and material characteristics: hydraulic bulge testing of tubes, Journal of Materials Processing Technology 98 (2000) 34-40
- [12] Koç M, Aue-u-lan Y, Altan T, On the characteristics of tubular materials for hydroforming – experimentation and analysis, International Journal of Machine Tools & Manufacturing 41 (2001) 761-772
- [13] Hwang YM, Lin YK, Analysis and finite element simulations of the tube bulge hydroforming process, Journal of Materials Processing Technology 125-126 (2002) 821-825
- [14] Strano M, Altan T, An inverse energy approach to determine the flow stress of tubular materials for hydroforming applications, Journal of Materials Processing Technology 146 (2004) 92-96
- [15] Bortot P, Ceretti E, Giardini C, The determination of flow stress of tubular material for hydroforming applications, Journal of Materials Processing Technology 203 (2008) 381-388
- [16] Lianfa Y, Cheng G, Determination of stress-strain relationship of tubular material with hydraulic bulge test, Thin-Walled Structures 46 (2008) 147-154
- [17] Vitu L, Boudeau N, Malécot P, Michel G, Buteri A, Evaluation of models for tube material characterization with the tube bulging test in an industrial setting, International Journal of Material Forming 11(5) (2018) 671-686
- [18] Abdelkefi A, Boudeau N, Malécot P, Michel G, Guermazi N, On the friction effect on the characteristics of hydroformed tube in a square section die: analytical, numerical and experimental approaches, Key Engineering Materials 639 (2015) 83-9